PHYSICAL REVIEW E

STATISTICAL PHYSICS, PLASMAS, FLUIDS, AND RELATED INTERDISCIPLINARY TOPICS

THIRD SERIES, VOLUME 52, NUMBER 1 PART B JULY 1995

ARTICLES

Video microscope and elastic light scattering studies of fast-mode kinetics in surface-mediated spinodal decomposition

Christopher Harrison*
Department of Physics, Princeton University, Princeton, New Jersey 08544

William Rippard
Department of Applied Physics, Cornell University, Ithaca, New York 14853

Andrew Cumming
Department of Physics, University of Florida, Gainesville, Florida 32611
(Received 10 November 1994)

We present time-resolved video microscope and elastic light scattering studies of the domain-pattern selection and growth of spinodal decomposition in critical mixtures of guaiacol and glycerol-water constrained to a cell 0.5 mm thick. The structure functions show two peaks with different kinetics: a slow mode with $L(t) \sim t^{1/3}$ and a "fast mode" with $L(t) \sim t^{b}$, where b ranges from 1.0 to 1.5 depending on the quench depth ($0.03\,^{\circ}\mathrm{C} \leq \Delta T \leq 0.35\,^{\circ}\mathrm{C}$). In this study we discuss our observations of the fast mode's growth. We have used both elastic light scattering and direct visualization via video microscopy and digital image processing to study the morphology and kinetics of these structures. Parameters such as the quench depth and the treatment of the cell's windows have been varied, with results suggesting that domain growth proceeds with a power law that is independent of which phase wets the surface.

PACS number(s): 68.45.−v, 05.70.Ln, 64.60.−i

I. INTRODUCTION

The process of phase separation has been observed in a variety of quenched systems with two or more components. As well as being scientifically interesting, this phenomenon is increasingly important for the manufacture and production of new materials, motivating us to seek a comprehensive understanding of the dynamics of phase separation. Investigations of alloys [1], critical binary fluids [2], and polymer mixtures [3–5] have yielded a fairly complete understanding of the bulk, three-dimensional pattern selection and growth in phase-separating binary fluid systems. Significant problems still remain, however, such as an understanding of the kinetics of spinodal decomposition near a surface following a quench. In this experiment, we address this problem with studies of a quasibinary fluid system.

Previous work on binary polymer mixtures has described two distinct phase-separation modes [6] following a temperature quench from the single-phase, thermodynamically stable region into the thermodynamically unstable region. In addition to the familiar bulk mode (or *slow mode)* [7], a different mode with much faster kinetics was observed in recent experiments in polymer blends, referred to as the fast mode [6]. To establish the generality of this fast mode to binary fluids, elastic light scattering studies in the simple liquid mixture guaiacol–glycerol-water (GGW) have been recently undertaken, and a similar fast mode has been observed and characterized [8].

In order to gain further understanding of the fast mode, we were motivated to study both the morphology of the fast-mode structures and the kinetics of phase separation in GGW. We found video microscopy to be a beneficial technique to study the developing structure function of a quenched sample. In addition to making observations of the morphology of the structures, in this paper we compare data from both elastic light-scattering and video microscopy studies, showing corresponding re-

*Author to whom correspondence should be addressed.

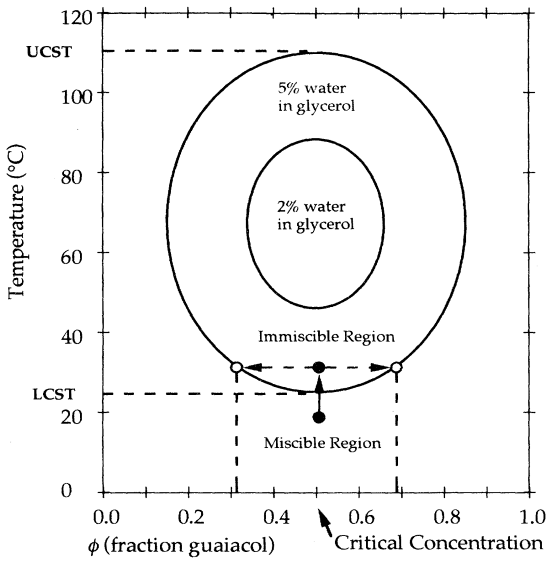

FIG. 1. Phase diagram for the quasibinary fluid guaiacol–glyercol-water (GGW). The upper critical solution temperature (UCST) and lower critical solution temperature (LCST) are approximately 110 °C, and 25 °C respectively. The arrows trace a quench from the one-phase miscible region into the two-phase immiscible region. The two resulting phases from a quench are comprised of the guaiacol fractions specified by the two points on the larger oval.

sults by the two techniques. We also present evidence that domain growth proceeds with the same power law dependence regardless of which phase is wetting the surface. Lastly, we compare our observations to Troian's recently proposed theory concerning the fast mode [9,10].

II. DESCRIPTION OF THE QUASIBINARY SYSTEM

Pure glycerol and guaiacol are miscible, but with the addition of a small amount of water (as little as 1.4% of the mass of glycerol) a miscibility gap opens (Fig. 1). The added water is absorbed by the hygroscopic glycerol, but it is almost immiscible with guaiacol. The system can be regarded as binary with glycerol-water as one component and guaiacol as the other. For systems with 5% water in glycerol or greater, GGW exhibits Ising-like critical exponents, as described elsewhere [11,12]. The closed-loop phase diagram has both an upper critical solution temperature and a lower critical solution temperature (UCST and LCST) which are the highest and lowest temperatures, respectively, at which the system phase separates. These temperatures are very sensitive to water content. Outside of the miscibility gap, GGW is in a single-phase state and mixes, but within the gap the GGW is immiscible and demixes into two phases. Our samples are initially below the LCST and we quench a few tenths of a degree into the miscibility gap above the LCST to demix. In our GGW samples, the water ratio was slightly greater than 5% in order to set the LCST (T_c) to about 26 °C.

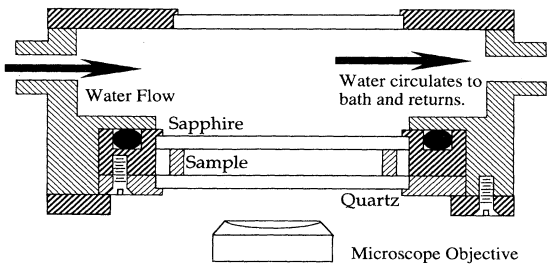

FIG. 2. The sample carrier. Thermally regulated water circulates through the carrier, in direct contact with the sample cell. The carrier rests on the microscope's stage.

III. EXPERIMENTAL APPARATUS AND OPERATION

Our sample cell consists of a Teflon gasket sandwiched between glass and sapphire windows containing a few drops of GGW (Fig. 2). This cell is then mounted in a sample carrier through which thermally regulated water circulates (warm bath stability of ±3 mK, cool bath stability of ±5 mK). The temperature of the cool bath is controlled by a Neslab RTE-220, and additional stability is obtained for the warm bath by a combination of a Neslab bath and a Lakeshore DRC-93C temperature controller. The Lakeshore reads the warm bath's temperature with a Yellow Springs Instrument Co. thermistor (30 000 Ω at 25 °C) and further stabilizes the bath's temperature with a heater. Two four-way ball valves control which bath's water circulates through the cell carrier. Before a quench, we *anneal* the cell at a temperature 10 mK below T_c by circulating the cool bath water through the carrier. To quench the sample by abruptly raising the temperature, we quickly switch the ball valves to reroute the cool bath water away from the carrier and the warm bath water through it, with a characteristic time of 6 sec for temperature increase. The sample, which was initially in the miscible state, is quenched above the LCST into the miscibility gap by the temperature increase. The quench depth, $\Delta T = T_f - T_c$, where T_f is the sample's final temperature as measured by the thermistor, is controlled by our temperature setting for the warm bath. Following the quench, the system demixes, allowing us to study the kinetics and the structures of the phase separations as the two phases are driven to separate. After we have finished our observations, we reroute the cool bath water to the carrier and allow the sample to anneal.

We have previously published a description of our light scattering apparatus [8], but not our video microscope. For microscopy studies, the sample carrier is mounted on a Zeiss Axiovert 35 inverted-axis microscope with sufficient magnification objectives (32×, 10×, and 2.5×) to study phase-separation morphology during demixing from micrometer-sized structures to structures on the order of several millimeters. The depth of focus (the range over which the image remain in adequate focus) is smaller for the more powerful magnification such that the 32× objective has a small depth of focus (~50 μm), but the 2.5× objective has a depth of focus which is larger (~200 μm).

The microscope's condenser focuses the light on the focal plane of the sample. The refraction index mismatch (about 0.01) of the two phases bends the light at the inter-

face boundaries, creating the image. The structures that we examine are large enough to be seen clearly at the magnification we have available, but the slight index mismatch allows only a low contrast, which we enhance by constricting our condenser iris to the setting for the smallest opening. The condenser's iris setting is a tradeoff between maximum resolution, with it completely open (iris diameter of 34 mm), and maximum contrast, with is almost closed (iris diameter of 1 mm). The latter setting for the condenser has a numerical aperture (NA) setting of approximately 0.02, much smaller than the nominal NA for our microscope's objectives.

By installing actuators to control the cell on the microscope's stage, we can focus the microscope on any volume of the cell. We attached a Newport 495-A computer controlled rotation stage to the microscope's focus knob to accurately control the microscope's focal plane with a resolution of 3 μm (z direction). By attaching two Newport 850-A linear actuators to the carrier's micropositioners, we also have control in the x,y directions parallel to the microscope stage with resolution of 6 μm. A three-axis Newport PMC300 power interface plugged into an IBM PC-compatible computer controls these postioners.

A Hitachi KP-140 charge coupled device (CCD) video camera, with 256 gray levels (8 bits) of dynamic range, is mounted on the microscope, enabling us to view the microscope's image on a monitor. During an experiment, we record this signal on a Sony SLV-686HF videocassette recorder to facilitate examination of the data at a later time. For a typical quench, the computer digitized about 45 time-sequenced images of phase separation from the videotape. Fifteen images are usually digitized for each of the three objectives, for this appears to be sufficient to characterize the growth of the structures, $L(t)$. For the 32× objective, the structures will quickly grow to exceed the screen size within a minute, so that we record images every 2 to 3 sec. At later times, the 2.5× objective allows for at least 15 min of structure growth, requiring us to sequence our images at one per minute.

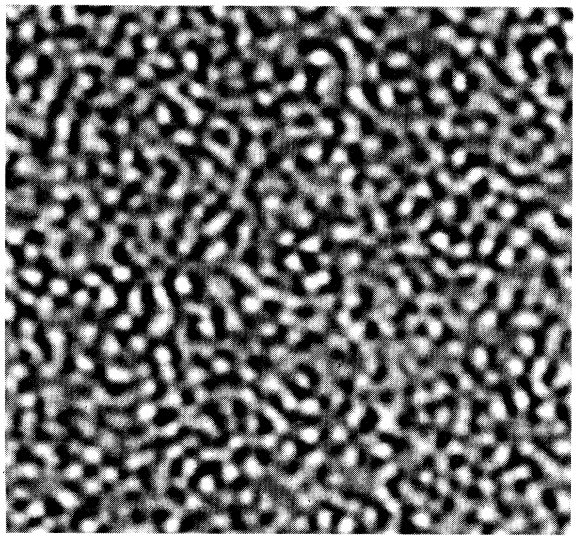

FIG. 3. Phase separation of a *critical* GGW mixture (T_c of 25.25 °C, quench depth of 0.2 °C, 15 sec after quench) is shown as viewed with the microscope's 32× objective, $c(\mathbf{r})$. Image width is 100 μm.

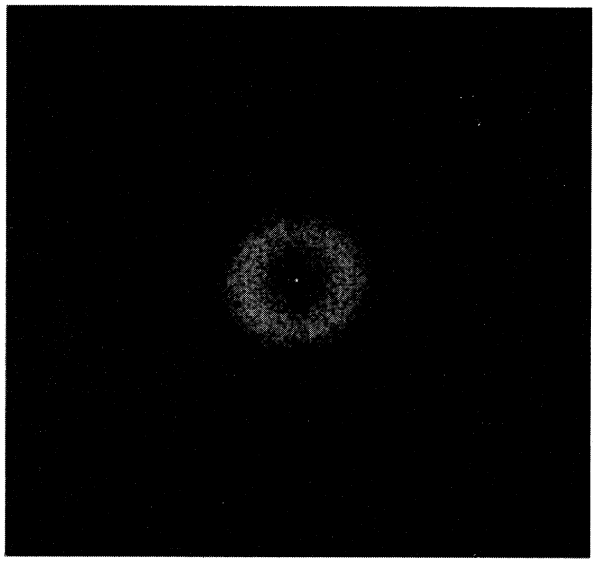

FIG. 4. Absolute square of the Fourier transformation on Fig. 3 is shown, $|c(\mathbf{q})|^2$.

Within 5 sec after a quench, the phase separation as seen through the 32× microscope objective appears as isotropic modulations with a characteristic length scale in the optical density function $c(\mathbf{r},t)$ (Fig. 3). The absolute square of the Fourier transform (Fig. 4), $|c(\mathbf{q},t)|^2$, where $c(\mathbf{q},t)$ is the Fourier transform of $c(\mathbf{r},t)$, corresponds to the elastic light scattering's structure function, $S(\mathbf{q},t)$ [2]. In light scattering, the structure function is produced by scattering from the small domains in the sample. Similarly, these refraction index modulations give rise to the image we see in the microscope. By Fourier-transforming these images, and squaring, we are

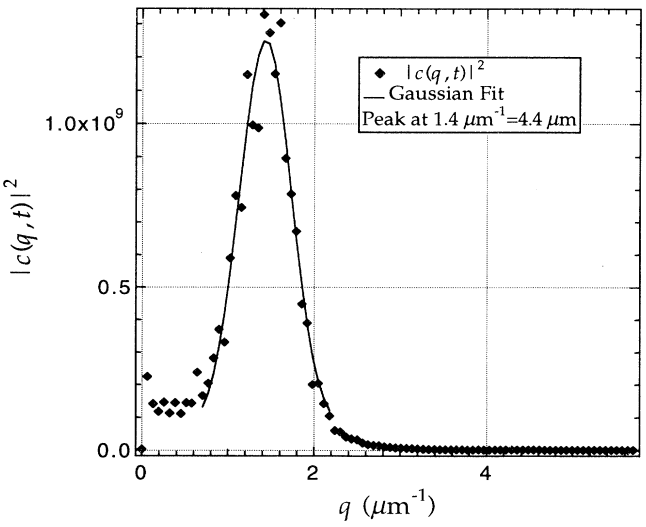

FIG. 5. Data shown are the azimuthal average of Fig. 4, plotted against the radius q, which clearly shows a peak at 4.4 μm. The data are fitted with a Gaussian function.

performing an operation similar to light scattering, and in both cases we see a ring whose radius corresponds to the average length of the phase-separating structures. A similar technique has been described elsewhere [13].

The phase-separation images are Fourier-analyzed using Image Processing Lab by Signal Analytics. These time-resolved Fourier transforms are batch processed by the computer to obtain the average size of the phase-separation structures for each image. The computer takes the points in q space, to $|c(\mathbf{q},t)|^2$, and azimuthally averages the points at each q radius from the center to obtain $|c(q,t)|^2$, which can be directly compared to the light scattering structure function $S(q,t)$. Figure 5 shows $|c(q,t)|^2$, which the IP Lab routine extracts from the data of Fig. 3. Whereas Furukawa [14] has proposed a dynamical structure function for the bulk mode, no such theoretical framework is yet available to our knowledge for the fast mode. Therefore we use a Gaussian to fit our fast-mode data because its form is similar to our structure functions. The fast-mode data are fit with a Gaussian (1) to obtain the fitted q value for our data, q_m. The fit function is

$$S(q)=S_0+S_1\exp\left[-\frac{(q-q_m)^2}{2\sigma^2}\right], \tag{1}$$

where S_0, S_1, q_m, and σ are the parameters of the least squares fitting routine. After obtaining q_m from the fit, we relate l_m to q_m in the usual way:

$$l_m=\frac{2\pi}{q_m}. \tag{2}$$

Figure 5 shows the Gaussian fit to the sample digital structure function from Fig. 3. The fit yielded a q_m of 1.4 μm^{-1}, corresponding to an average length (l_m) of 4.4 μm. Figure 6 shows an example of several time-sequenced $|c(q,t)|^2$ functions with q_m decreasing as the average size of the phase-separation structures grows.

As we will address in Sec. V, the fast mode and slow mode are normally seen at different planes in the sample. Because the microscope focuses on one plane of the sample, we can examine only one mode of phase separation at a time with the video microscope. However, light scattering measures phase separation along all planes of the sample as the beam does not focus on any particular spot. Previously published light scattering data by our group shows $S(q,t)$ which contains structure from both the fast mode and the slow mode [8]. Our data from the video microscope in Fig. 6 shows structure only from the fast mode, as the microscope is focused on the fast-mode plane during the experiment, and cannot measure the slow-mode signal without focusing on the slow-mode plane. However, the video microscope can see both modes concurrently if the depth of focus is quite large by using a low magnification, as in Fig. 8(d). At this low magnification, unfortunately we cannot sufficiently characterize the structure function to take reliable data.

Three sections of the data during the structure growth are taken with the microscope set on an objective of sequentially decreasing magnification. This is necessary to obtain a sufficient number of modulations in the optical density function across the microscope's image to obtain an accurate Fourier transform.

Finally, we can visualize $L(t)$, the average size of the structures as a function of time, by plotting l_m versus time for our video microscopy data. It is found that $L(t)\sim t^b$, where b is our kinetic exponent. Note that this is consistent with our previous light scattering results, where we found $q_m\sim t^{-b}$ [8]. An example of $L(t)$ for a quench depth of 0.19 °C (acid-cleaned sample cell, video microscopy data) is shown in Fig. 7 which suggests that a power law is obeyed with $L(t)\sim t^{1.37}$ for the early stages of phase separation. Taken alone, this video microscopy data suggests, but does not prove, that a power a law is obeyed, for the range of domain growth is slightly less than an order of magnitude for both axes. Similarly, the data suggest a turnover to linear growth at later times.

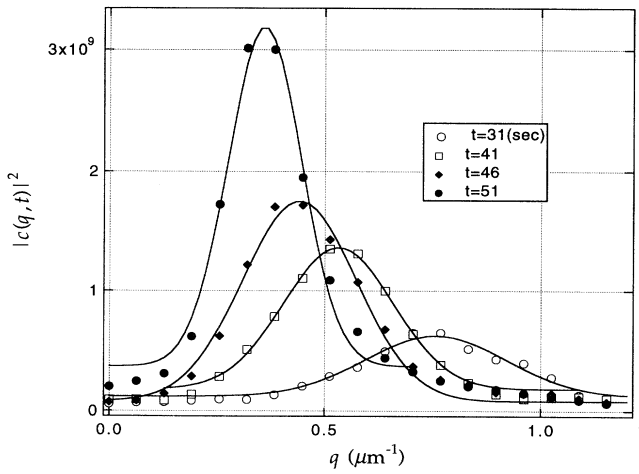

FIG. 6. Time-resolved $|c(q,t)^2$ from the video microscope are shown as an example of the coarsening structure function after a quench (T_c of 23.6 °C, depth of 0.1 °C, times of 31, 41, 46, 51 sec). As the average size of the phase-separating structures grows, the peaks move to lower q.

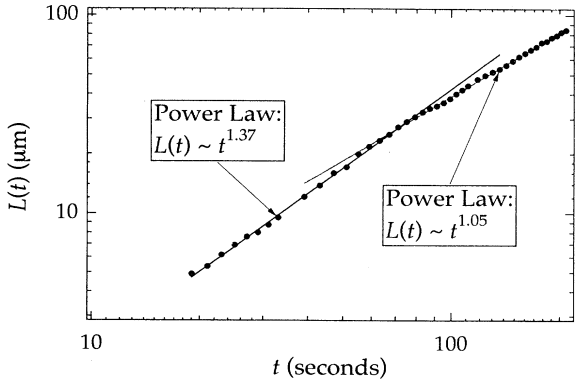

FIG. 7. An example of $L(t)$ from the video microscope for a critical mixture of GGW, quench depth of 0.19 °C, where $L(t)\sim t^{1.37}$ during the early stage. The sample cell has been acid cleaned. The line corresponds to a function proportional to $t^{1.37}$. Note that at the late stage there is a turnover to linear growth.

This will be treated in Sec. VI.

We found video microscopy to be an advantageous tool for studying phase separation. Though the data were not as precise as those of light scattering, it enabled us to study the morphology of phase separation while simultaneously obtaining the structure function. Video microscopy also allowed us to study the structure function up to an average domain size of 100 μm, whereas our light scattering apparatus had a maximum size limit of 25 μm. Deep quenches produce a structure function which quickly time evolves and can be studied best with the ability to follow it to larger length scales. The video microscope's ability to do this enabled us to determine the kinetic exponents of deeper quenches than was possible with light scattering.

IV. SAMPLE CELL SURFACE TREATMENT

We investigated two different types of sample cells: those whose windows were acid-cleaned and those whose windows were treated further with a surface altering monolayer. Glycerol has a higher affinity than guaiacol for the hydrophilic windows of the acid-cleaned cell. The surfaces of the treated cells were altered with a monolayer of phenethyl trichlorosilane to make the glass hydrophobic; the guaiacol then had the higher affinity. This was confirmed with capillary-rise experiments. During demixing, we believe that the glycerol-rich phase is wetting the surface for the untreated cells and the guaiacol-rich phase is wetting the surface of the treated cell.

V. OBSERVATIONS OF FAST MODE'S MORPHOLOGY

Observations of the fast mode's morphology were primarily made with our microscope. The sample was agitated while annealing below T_c to allow the GGW to mix homogeneously. After annealing the sample for days, we observed after quenching that the fast mode grew on the top and bottom windows of the cell in 50 μm thick regions, as one would expect for a surface-driven phenomenon. For such quenches, the bulk mode would predominantly be in the center of the cell. We note that this is slightly different than the 10 μm thick region observed in the polymer system [5].

After performing a deep quench [$\Delta T = 0.2\,^{\circ}$C, with the domain size up to $L(t) \sim 100\mu$m] an anneal time of up to three days was required to homogenize and thoroughly remix the system. Shorter anneal times prior to requenching resulted in a fast mode on the next quench with different characteristics than described in the preceding paragraph. This different fast mode was approximately 150 μm thick and predominantly in the lower half of the sample cell, suggesting that gravity played some role. However, phase separation proceeded

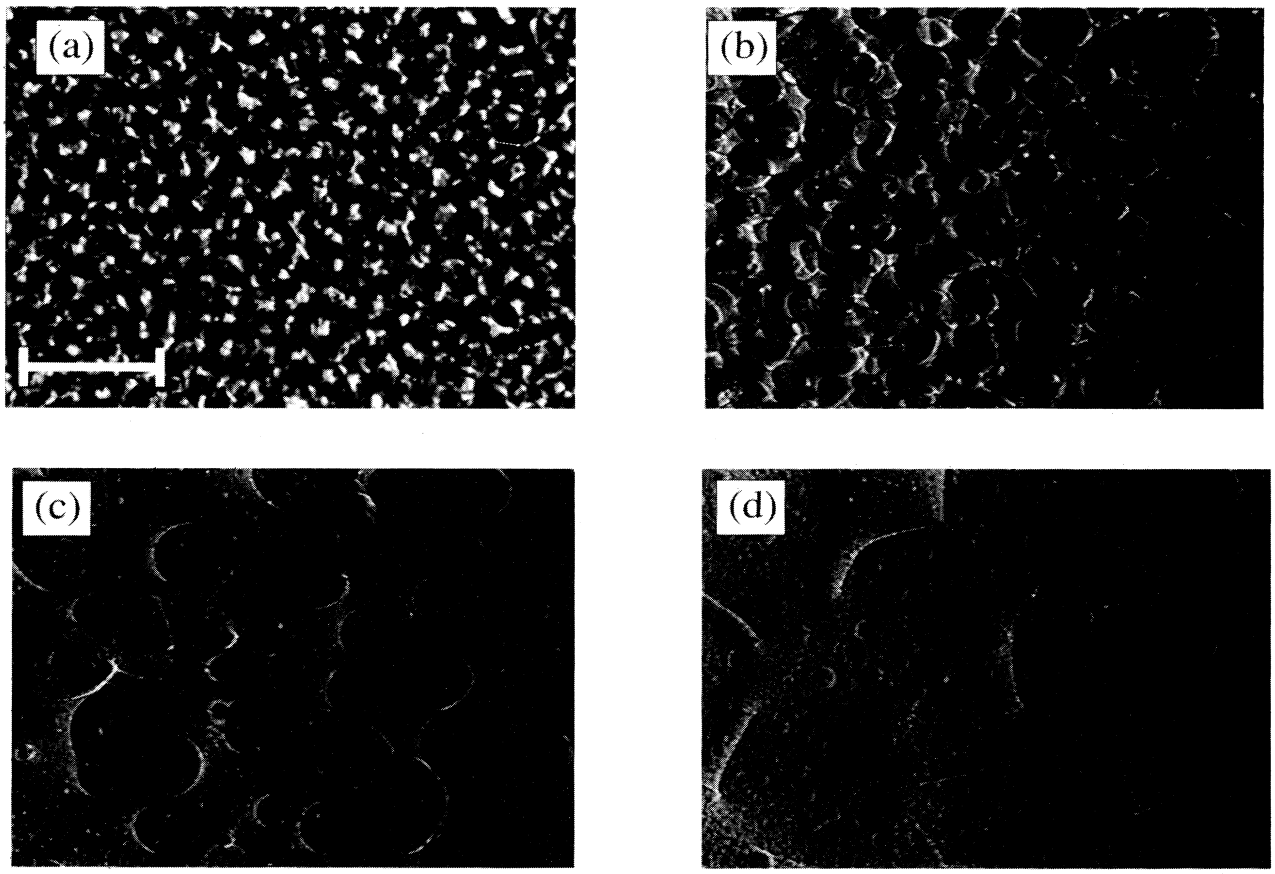

FIG. 8. Four pictures of structure growth (T_c of 24.9 °C, depth of 0.1 °C, times after quench of 30, 162, 380, 440 sec) close to the cell's surface, taken with the 10× objective on the Zeiss microscope. The bar corresponds to 200 μm.

at the same rate regardless of the location of the fast mode in the cell, and for most data acquisition the fast mode was in this 150 μm thick layer in the lower portion of the cell.

Observations suggest that wetting by one phase on the cell window plays an important role in fast-mode phase separation. The four images of Fig. 8 show growth of the fast mode along the surface of the cell window, starting with the small structures of Fig. 8(a) ($\sim$4 μm) to the larger structures in Figs. 8(c) and 8(d). The phase-separation domains of Fig. 8(a) can be resolved within 5 sec after a quench. Moving the focal plane up and down 10 μm allows one to focus on different planes and hence different domains, but the image changes little as long as the focal plane is inside the approximately 50 μm thick spinodal decomposition matrix covering the window surface. As the phase separation continues, the phase separation seems to thin and the structures appear as overlapping domains, with some of the structures closer to the window and some structures farther away from the window [Fig. 8(b)]. These relative positions can be determined by moving the focal plane up and down by 10–20 μm and noticing which structures are in focus. As the average length of the domains as measured parallel to the window grows to 200 μm or larger, the growth *appears* to be a wetting phenomenon with some protuberant structures protruding from the windows's surface and some structures resulting from the absence of the wetting phase along the window, particularly noticeable with schlieren illumination in Fig. 8(c). Figure 8(d) shows the last remnants of the fast mode within 20 μm of the cell window. The disappearing structure of the fast mode along the window surface during the late stage fits the pattern of one phase completely wetting the surface. The smaller circles in the background can be attributed to bulk phase separation which grows much more slowly than the fast mode.

VI. RESULTS

By use of the previously described Fourier analysis, we were able to measure the average size L of the fast-mode structures using video microscopy. We were also able to measure $q_m(t)$ via elastic light scattering with the setup that was reported previously [8]. For video microscopy, the fast-mode kinetics were found to follow a power law, with $L(t) \sim t^b$ ($1.0 < b < 1.5$, $0.03\,^{\circ}\mathrm{C} \leq \Delta T \leq 0.35\,^{\circ}\mathrm{C}$) where b varies depending upon the quench depth. Similarly, we measured $q_m(t) \sim t^{-b}$ with our light scattering apparatus for a slightly smaller temperature range. The range of video microscopy data was from approximately 4 to 100 μm and for light scattering the range was from 0.1 to 25 μm. These ranges were designed to allow light scattering to study small structures at early times and for the video microscope to study the larger structures as they became macroscopic. The data showing the dependence of the kinetic exponent (b) on the quench depth by our two independent experimental techniques of light scattering (LS) and video microscopy (VM) are plotted together in Fig. 9.

We first compared our light scattering and video microscopy data from acid-cleaned sample cells, finding

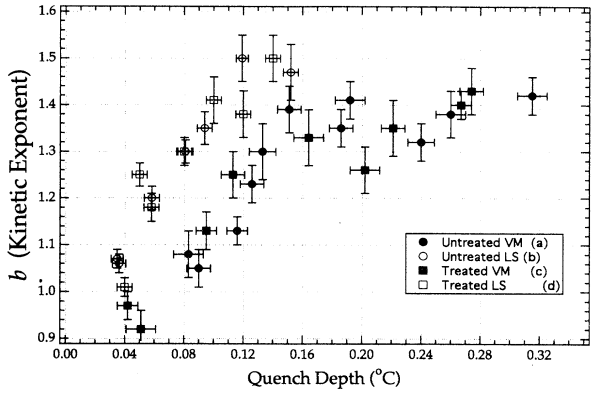

FIG. 9. Kinetic exponent (b) dependence on quench depth. Data sets (a) and (b) refer to video microscopy (VM) and light scattering (LS) data, respectively, using sample cells whose surfaces were not treated. Data sets (c) and (d) refer to VM and LS data, respectively, using sample cells whose surfaces were treated with a monolayer of phenethyl trichlorosilane. Note that the solid data points are those of VM and the outlined data points are those of LS.

that they each follow the same trend: the kinetic exponent increases from about 1.0 for a shallow quench to 1.5 for a deep quench [data sets (a) and (b) in Fig. 9] within a temperature range of 0.04 °C to 0.15 °C. Due to its ability to handle larger length scales, video microscopy enabled us to quench deeper than our light scattering apparatus could, and we found from this that b maintained a value of about 1.4 for quench depths greater than 0.15 °C to the deepest quenches of 0.32 °C. Though the data sets are generally in agreement, there is an offset from the light scattering data to the video microscopy data of about 0.04 °C. This offset is most likely due to the difference in measuring T_c by the two experiments. We believe that we measured the video microscope's T_c to be lower than that of light scattering, which would indeed make the video microscope's quenches appear to be deeper for a given kinetic exponent.

An additional source of error is that the two experimental procedures are in fact measuring slightly different signals: light scattering is a three-dimensional bulk measurement, whereas video microscopy performs a two-dimensional fast Fourier transform (FFT) on a "slice" of the fast mode as seen through the microscope. Figure 9 shows that for LS, the largest value of the kinetic exponent is $b=1.5$, whereas VM reports the largest value as $b=1.4$. Because we saw this discrepancy in many experiments, we believe that this discrepancy was systematic and the result of the different signals that the two experiments measured.

Within experimental error, the data sets for the sample cells which were treated with phenethyl trichlorosilane [data sets (c) and (d) of Fig. 9] show no difference from those of the cells that were acid cleaned [data sets (a) and (b)]. Our hypothesis is that the glycerol-rich phase is wetting the surface for the untreated cells and the guaiacol-rich phase is wetting the surface of the treated cell, but regardless of the phase which is wetting, the same kinetics result. These data suggest that some other

surface mechanism besides a monolayer of polymers should be employed to affect the fast mode in an experimentally verifiable manner.

At the late stages of our video microscopy experiments, with $L(t) \sim 40-100$ μm, we see a turnover of b from $b > 1$ to $b \sim 1$ (Fig. 7). We cannot see this with light scattering because 25 μm is the upper limit of our structure function resolution, and the light scattering data closely follow the power law growth through the range of the data (0.1–25 μm). All video microscopy experiments at different quench depths display this turnover, though it becomes more difficult to see for the shallow quenches, for if b is approximately 1 during the early stage, a turnover of b to 1 becomes difficult to resolve. The later part of this data appears to be linear with time, but as mentioned previously the range is too narrow to establish it with absolute certainty. This turnover to linear growth was predicted by Siggia by taking hydrodynamic flow into account [14–16].

Theorists are currently working on models to understand the fast mode's driving mechanism. The work of Rogers, Elder, and Desai which describes droplet growth and coalescence on a surface theorizes that growth by coalescence has a kinetic exponent which is three times that of the growth through diffusion alone [17]. Troian has argued that Rogers's work relates as well to phase separation, which when applied to previous work on the fast mode produces a kinetic exponent between 1 and 1.5, dependent on quench depth [9,10]. The kinetic exponent generated by this theory is in agreement with our results.

Troian's work also suggests that domain growth should proceed at the same rate regardless of which phase is wetting the sample cell's surface. As mentioned previously, our data support this since we obtained similar kinetic exponent dependence on quench depth for both the acid-cleaned and surface-modified sample cells, which we believe have opposite phases wetting the surface.

ACKNOWLEDGMENTS

This work was supported by the NSF-PYI program, AT&T, and Exxon. We gratefully acknowledge the assistance of Bill Shi and Wade Robinson.

[1] K. Hono and K. I. Hirano, Phase Transitions **10**, 223 (1987).
[2] W. I. Goldburg, in *Light Scattering Near Phase Transitions,* edited by H. Z. Cummins and A. P. Levanyuk (North-Holland, Amsterdam, 1983).
[3] T. Hashimoto, Phase Transitions **12**, 47 (1988).
[4] F. S. Bates and P. Wiltzius, J. Chem. Phys. **91**, 3258 (1989).
[5] A. Cumming, P. Wiltzius, F. S. Bates and J. F. Rosedale, Phys. Rev. A **45**, 885 (1992).
[6] P. Wiltzius and A. Cumming, Phys. Rev. Lett. **66**, 3000 (1991).
[7] David A. Huse, Phys. Rev. B **34**, 7845 (1986).
[8] B. Shi, C. Harrison, and A. Cumming, Phys. Rev. Lett. **70**, 206 (1993).
[9] S. M. Troian, in *Dynamics in Small Confining Systems,* edited by J. M. Drake *et al.,* MRS Symposia Proceedings No. 290 (Materials Research Society, Pittsburgh, 1993).
[10] S. M. Troian, Phys. Rev. Lett. **71**, 1399 (1993).
[11] Roger G. Johnston, Noel A. Clark, Pierre Wiltzus, and David S. Cannell, Phys. Rev. Lett. **54**, 49 (1985).
[12] R. G. Johnston, N. A. Clark, P. Wiltzius, and D. S. Cannell, Phys. Rev. Lett. **54**, 49 (1985); R. G. Johnston, *Investigation of Closed-Loop Miscibility Curves* (UMI Dissertation Services, Ann Arbor, 1983).
[13] P. Guenoun, R. Gastaud, F. Perrot, and D. Beysens, Phys. Rev. A **36**, 4876 (1987).
[14] H. Furukawa, Physica A **123**, 497 (1984).
[15] Eric D. Siggia, Phys. Rev. A **20**, 595 (1979).
[16] Y. C. Chou and Walter Goldburg, Phys. Rev. A **20**, 2111 (1979).
[17] T. M. Rogers, K. R. Elder, and Rashmi C. Desai, Phys. Rev. A **38**, 5303 (1988).

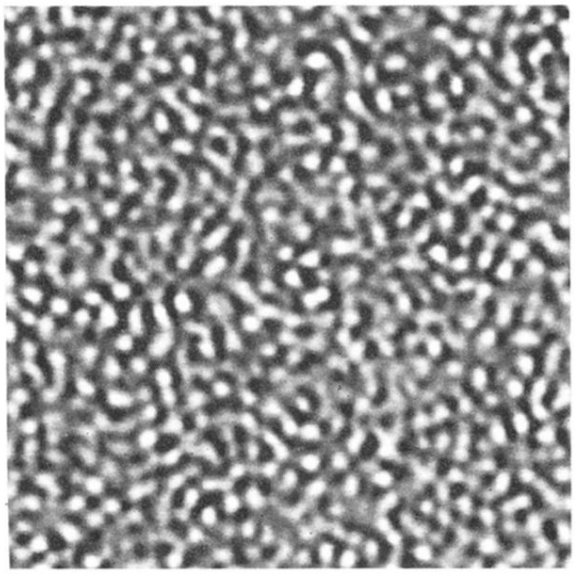

FIG. 3. Phase separation of a *critical* GGW mixture (T_c of 25.25 °C, quench depth of 0.2 °C, 15 sec after quench) is shown as viewed with the microscope's 32× objective, $c(\mathbf{r})$. Image width is 100 μm.

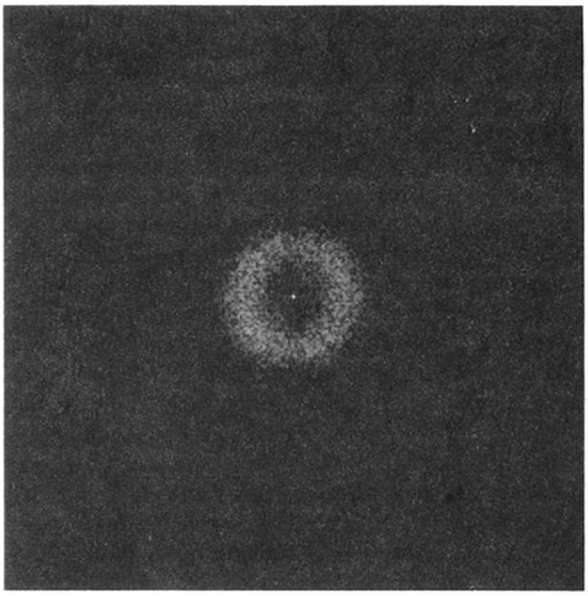

FIG. 4. Absolute square of the Fourier transformation on Fig. 3 is shown, $|c(\mathbf{q})|^2$.

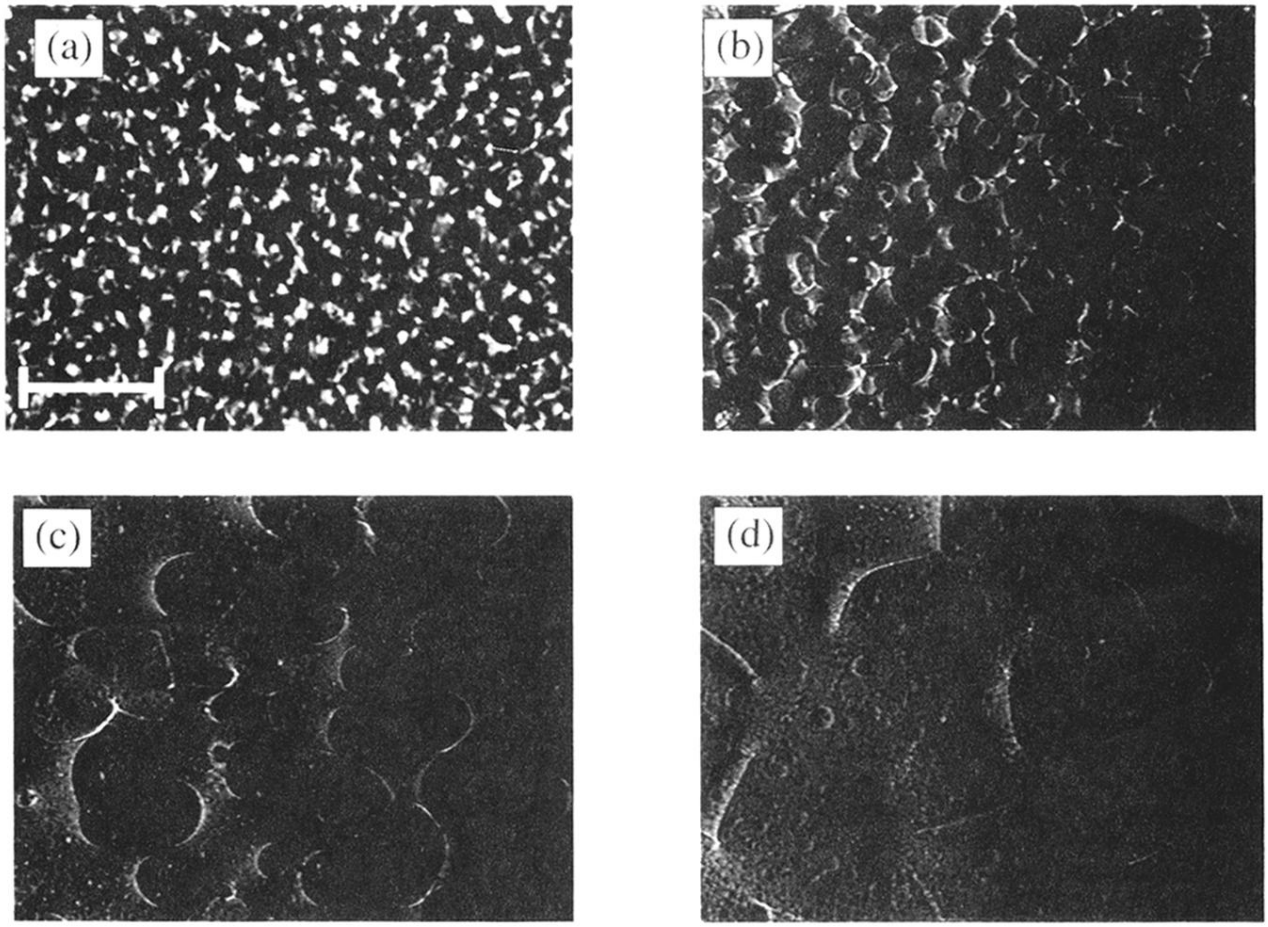

FIG. 8. Four pictures of structure growth (T_c of 24.9 °C, depth of 0.1 °C, times after quench of 30, 162, 380, 440 sec) close to the cell's surface, taken with the 10× objective on the Zeiss microscope. The bar corresponds to 200 μm.